Langmuir

Article

pubs.acs.org/Langmuir

Exploiting the Wall-Induced Non-inertial Lift in Electrokinetic Flow for a Continuous Particle Separation by Size

Xinyu Lu,[†] Jyh-Ping Hsu,*[,‡] and Xiangchun Xuan*[,†]

[†]Department of Mechanical Engineering, Clemson University, Clemson, South Carolina 29634-0921, United States

[‡]Department of Chemical Engineering, National Taiwan University, Taipei 10617, Taiwan

ABSTRACT: Separating particles from a heterogeneous mixture is important and necessary in many engineering and biomedical applications. Electrokinetic flow-based continuous particle separation has thus far been realized primarily by the use of particle dielectrophoresis induced in constricted and/or curved microchannels. We develop in this work a new electrokinetic method that exploits the wall-induced non-inertial lift in a straight uniform microchannel to continuously separate particles by intrinsic properties (e.g., size and surface charge). Such an electrically originated lift force arises from the asymmetric electric field distribution around a particle nearby a planar dielectric wall. We demonstrate this method through separating both a binary and ternary mixture of dispersed polystyrene microspheres by size in a T-shaped microchannel. A semi-analytical model is also developed to simulate and understand the particle separation process. The predicted particle trajectories in the entire microchannel agree reasonably well with the experimental measurements.

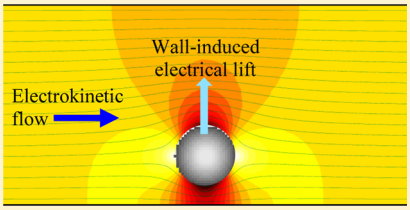

INTRODUCTION

Separating particles from a heterogeneous mixture is important and necessary in many engineering and biomedical applications. Microfluidic devices have been increasingly used in the past 2 decades to achieve this function because of their enhanced efficiency at a reduced cost and other advantages as well.[1−5] Electrokinetic flow is an efficient means to transport fluids and particles in these devices and possesses a desirable nearly flat velocity profile compared to the traditional parabolic hydrodynamic flow.[6,7] For the latter pressure-driven flow, an extra force field (e.g., electrical,[8] optical,[9] acoustic,[10] magnetic,[11] and hydrodynamic[12] forces) can be externally imposed to directly manipulate particles for an active separation. Alternatively, introducing fluid inertia[13,14] and/or obstacles[15,16] into pressure-driven flows through microchannels can cause cross-stream particle motions for a passive separation. In contrast, electrokinetic flow-based continuous particle separation has been realized primarily using the internally induced particle dielectrophoresis (DEP) in constricted[17−21] and/or curved microchannels.[22−25]

In this work, we will demonstrate a continuous-flow electrokinetic separation of particles via the wall-induced non-inertial lift in a straight uniform microchannel. Such an electrically originated lift force results from the asymmetric electric field around a dielectric particle nearby a planar dielectric wall. It was first analyzed by integration of the Maxwell stress over the surface of the particle in Young and Li's theoretical paper,[26] which was used to accurately determine the small gap distance separating a spherical colloidal particle in electrophoretic motion from a planar non-conducting surface. The same force was also considered in another paper from Kang et al.[27] via an empirical formula to simulate the trajectory of an electrokinetically moving particle around an insulating hurdle in a straight microchannel. Later, Yariv[28] obtained a leading-order expression for this electrical lift force, which provides a positive demonstration of the drift away of a dielectric particle from a planar wall under the influence of a tangential direct current (DC) electric field. This result is consistent with that of a recent theoretical study by Zhao and Bau,[29] who also demonstrated the existence of an electrical force between a dielectric particle and an adjacent planar dielectric wall.

The DEP-resembled (DEP is defined as the translation of a particle in response to a non-uniform electric field existing in the absence of the particle[30]) lift force has been experimentally verified by Liang et al.[31,32] via the electrokinetic focusing of polystyrene particles in both the horizontal and vertical planes of a straight rectangular microchannel. It has also been confirmed by Yoda's group[33] through using evanescent wave-based particle-tracking velocimetry to study the distribution of polystyrene and silica particles along the wall-normal coordinate. Recently, this wall-induced electrical lift has been found by DuBose et al.[34] to yield a particle-size-dependent equilibrium position for electrokinetic particle motion through a spiral microchannel, which can be predicted by Yariv's formula[28] with good agreement. More recently, it has been used by Liang et al.[35] to control the gap of particle−wall separation for an experimental verification of the enhanced electrophoretic particle mobility near a solid wall.

We will exploit the wall-induced electrical lift to demonstrate, for the first time to our knowledge, a continuous-flow electrokinetic separation of particles by size in a T-shaped microchannel. A semi-analytical model based on Yariv's

Received: October 1, 2014
Published: December 18, 2014

DOI: 10.1021/la5045464
Langmuir 2015, 31, 620−627

formula[28] will also be developed to simulate the particle trajectory in the entire channel and understand the electrokinetic particle separation.

EXPERIMENTAL SECTION

Preparation of Microchannels and Particle Solutions. The T-shaped microchannel, as shown in Figure 1, was fabricated with

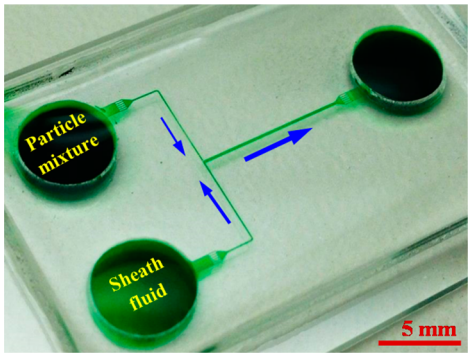

Figure 1. Picture of a T-shaped microchannel (filled with green food dye for clarity) with the arrows indicating the flow directions of the sheath fluid and particle mixture during the particle separation experiment.

polydimethylsiloxane (PDMS) using the standard soft lithography method. The detailed fabrication procedure can be referred to Lu et al.[36] The microchannel has a uniform depth of 40 μm, where the main branch is 1 cm long and 200 μm wide, while each side branch is 0.75 cm long and 100 μm wide. There are five rectangular blocks designed at each of the three reservoir−microchannel junctions, which are used to filter out PDMS debris and particle aggregates at the two inlets (for the sheath fluid and particle mixture, respectively, as indicated on the picture) and create six flow passages for separated particles at the outlet. The particle solutions were made by resuspending polystyrene spheres (Sigma-Aldrich, St. Louis, MO) of 5/10 μm (for a binary separation) or 3/5/10 μm in diameter (for a ternary separation) in 1 mM phosphate buffer to a final concentration of about 10^6 particles per milliliter. Glycerol (Fisher Scientific) was added to the buffer solution at a volume percentage of 22% to achieve neutral buoyancy for the suspended particles with a nominal density of 1.05 g/mL. It was found to also help suppress the particle adhesion problems. The dynamic viscosity of the particle solution was 1.908×10^{-3} kg m^{-1} s^{-1}.[37] The suspending medium of the particle solutions, i.e., 1 mM phosphate buffer with 22% (v/v) glycerol, was used for the sheath fluid (see Figure 1).

Particle Control and Visualization. The electrokinetic motion of particles in the microchannel was driven by DC electric fields, which were supplied by a DC power supply (Glassman High Voltage, Inc., High Bridge) and a function generator (3322A, Agilent Technologies) in conjunction with a high-voltage amplifier (609×10^{-6}, Trek). Pressure-driven fluid and particle motions were minimized by carefully balancing the liquid levels in the three reservoirs prior to each test and continuously running the experiment for no more than 5 min each. Particle transport and separation was visualized and recorded through an inverted microscope (Nikon Eclipse TE2000U, Nikon Instruments) with a charge-coupled device (CCD) camera (Nikon DS-Qi1Mc) at a rate of 20 frames per second. The obtained videos and images were post-processed using the Nikon imaging software (NIS-Elements AR 2.3). Particle streak images were obtained by superimposing a sequence of around 300 images. The electrokinetic particle mobility, i.e., electrokinetic velocity per unit electric field, was measured by tracking single particles in the microchannel. The three types of particles used in our experiment were found to have a similar electrokinetic mobility value of $\mu_{EK} = 1.1 \times 10^{-8}$ m^2 V^{-1} s^{-1} (cf. eq 1), which is consistent with the measurement in our earlier study.[32]

THEORETICAL SECTION

Mechanism of Particle Separation. In the absence of a particle, electric field lines (and, hence, fluid streamlines because of the similarity between the electric and velocity fields in pure electroosmotic flows[6,7]) in a fluid through a straight uniform microchannel are parallel to the walls and uniformly distributed. However, the presence of a finite-sized particle causes distortions to the electric field lines (and as well fluid streamlines), creating electric field gradients around it. This is evident from Figure 2A, which shows the electric field

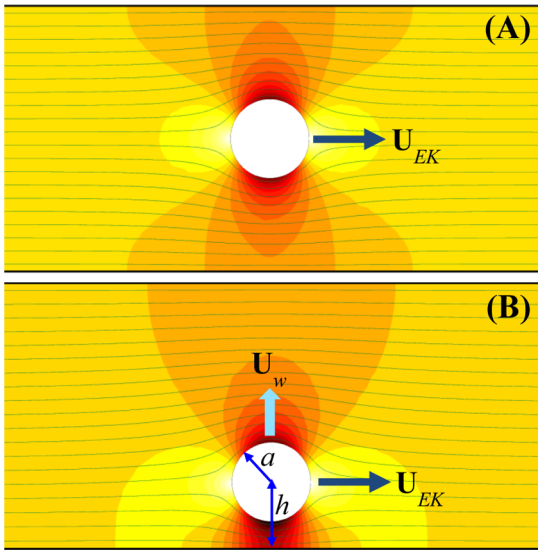

Figure 2. Illustration of the electric field lines (similar to fluid streamlines) and contour (the darker the color, the larger the magnitude) around a spherical particle in the horizontal planar of a straight rectangular microchannel when the particle is traveling electrokinetically (A) along the axis and (B) near one dielectric wall at a velocity, $\mathbf{U}_{EK}$. The particle in panel B drifts away from the wall at a velocity $\mathbf{U}_w$ because of a wall-induced electrical lift force that arises from the asymmetric electric field around it in the transverse direction.

lines and contour (the darker the color, the larger the magnitude) around a particle as it travels along the axis of a straight microchannel at an electrokinetic velocity of $\mathbf{U}_{EK}$ (a combination of fluid electroosmosis and particle electrophoresis)

$$\mathbf{U}_{EK} = \frac{\varepsilon(\zeta_p - \zeta_w)}{\eta} = \mu_{EK}\mathbf{E} \quad (1)$$

where ε is the fluid permittivity, ζ_p is the ζ potential of the particle, ζ_w is the ζ potential of the channel wall, η is the fluid dynamic viscosity, μ_{EK} is the electrokinetic particle mobility, and $\mathbf{E}$ is the applied axial DC electric field. Note that the wall-induced modification of $\mathbf{U}_{EK}$ is neglected in eq 1, which has been proven reasonable unless the particle closely fits the microchannel[38−40] or nearly touches a channel wall.[35,41,42] In the case of particle electrophoresis along the channel axis, the electric field distribution is symmetric about the particle in both the streamwise (i.e., axial) and cross-stream (i.e., transverse) directions, as seen from Figure 2A. Hence, there is no net electrical force, which can be accurately determined from the surface integral of the Maxwell stress tensor, acting on the particle.

DOI: 10.1021/la5045464
Langmuir 2015, 31, 620−627

In contrast, when a particle moves eccentrically in a straight microchannel near one of its dielectric walls, the electric field distribution around it becomes asymmetric in the transverse direction, as illustrated in Figure 2B. Hence, an electrical lift force acting on the particle is induced, driving it away from the wall. This force is different from the electric double layer force between two surfaces, which is significant only if the distance between the particle edge and the channel wall is on the order of nanometers.[43] It is also different from the so-called electroviscous lift, which is a force originating when a charged particle and its surrounding counterion cloud are made to move relative to each other near a wall.[44−46] Such a wall-induced lateral migration velocity, $\mathbf{U}_w$, for a spherical particle of radius a has been recently proposed by Yariv[28] to take the following form at the leading order:

$$\mathbf{U}_w = \frac{\varepsilon a \mathbf{E}^2}{32\mu}\left(\frac{a}{h}\right)^4 \mathbf{n} \tag{2}$$

where h is the perpendicular distance of the sphere center from the planar dielectric wall (see Figure 2B) and $\mathbf{n}$ is the unit normal to the wall pointing toward the fluid. It is important to note that eq 2 is only valid for remote sphere−wall interactions, i.e., $a/h \ll 1$. Moreover, the particle drift because of the inertial lift[13,14] is small compared to $\mathbf{U}_w$ in eq 2[29] as a result of the negligible inertial effects in electrokinetic flows,[6,7] where the channel Reynolds number is typically less than unity and the particle Reynolds number is far less than unity.[6,7]

The competition between the electrokinetic particle velocity, $\mathbf{U}_{EK}$ in eq 1 with a magnitude of U_{EK}, and the wall-induced particle drift velocity, $\mathbf{U}_w$ in eq 2 with a magnitude of U_w, results in a particle deflection across the fluid streamlines

$$\text{deflection} = \frac{L}{U_{EK}} U_w = \frac{a}{32}\left(\frac{a}{h}\right)^4 \frac{LE}{\zeta_p - \zeta_w} \tag{3}$$

where L is the lengthwise distance that the particle travels in the straight microchannel and E the magnitude of the applied DC electric field. Apparently, the deflection of a particle is a function of its size a and surface charge ζ_p; both are intrinsic particle properties. These dependences can be exploited to continuously separate a mixture of particles based on their size and/or surface charge. To do this, we use a sheath fluid to first pinch the particle suspension at the T junction of the microchannel (see Figure 1). Then, the focused particle stream starts being displaced from one sidewall of the main branch and is gradually split into two or more substreams (if more than two types of particles are present) along the channel length direction based on the particle size/charge-dependent deflection. Moreover, eq 3 indicates that increasing the electric field and/or using a long straight microchannel will enhance the particle deflection and, hence, improve the particle separation.

It is important to clarify the difference between our proposed method and the previously developed pinched flow fractionation (PFF) method via electroosmotic flow.[47] In the latter, particles of different sizes need to be first aligned against one sidewall of the pinched branch (i.e., the main branch of the T-shaped microchannel) by a strong sheath fluid. This alignment causes the centers of these particles to be located at different streamlines of the laminar electroosmotic flow because of steric effects;[48,49] i.e., the center of larger particles stays further away from the sidewall than that of smaller particles. Therefore, particles can be continuously separated on the basis of size by the spreading flow profile at the exit of the pinched branch. Several approaches have been developed to minimize the particle dispersion in PFF for an enhanced separation.[50−52] Also, a number of forces, such as optical force[53] and gravity,[54] have been demonstrated to increase the lateral displacement between particles of different sizes. In fact, the wall-induced electrical lift exploited in the current work is one such force that, however, is internally induced during electrokinetic particle motion and has no restrictions on particle density or charge.

Numerical Simulation of Particle Trajectories. We developed a Lagrangian tracking method based on a theoretical model in MATLAB (MathWorks) to simulate the particle trajectory.[27] The instantaneous position of the particle center $\mathbf{x}_p$ is obtained by integrating the particle velocity, $\mathbf{U}_p$, with respect to time t

$$\mathbf{x}_p = \mathbf{x}_0 + \int_0^t \mathbf{U}_p(t')\, dt' \tag{4}$$

$$\mathbf{U}_p = \mathbf{U}_{EK} + \mathbf{U}_w \quad \text{for particles in the main branch} \tag{5a}$$

$$\mathbf{U}_p = \mathbf{U}_{EK} + \mathbf{U}_{DEP} \quad \text{for particles in the other regions} \tag{5b}$$

In the above, $\mathbf{x}_0$ represents the initial location of the particle center and $\mathbf{U}_{DEP}$ is the velocity of particle DEP. For spherical particles in DC electric fields, $\mathbf{U}_{DEP}$ is given by[7,8,30]

$$\mathbf{U}_{DEP} = \frac{\sigma_p - \sigma}{\sigma_p + 2\sigma}\frac{2\varepsilon a^2}{3\eta}(E\nabla)E \tag{6}$$

where σ_p is the effective electric conductivity of particles and can be estimated from $\sigma_p = 2\sigma_s/a$, with $\sigma_s = 1$ nS being the surface conductance of a particle as suggested by Ermolina and Morgan.[56] It is important to note that $\mathbf{U}_{DEP}$ becomes non-zero only at the corners of the microchannel, where electric field gradients are locally induced by the curvature of the wall.[55]

The electric field, $\mathbf{E} = -\nabla\phi$, in the fluid was computed from a two-dimensional (2D) numerical model in COMSOL (COMSOL, Inc.), where the entire T-shaped microchannel, including the end-channel reservoirs, was included in the computational domain. Under the assumption of a thin electric double layer (typically on the order of nanometers[6,7]), the electric potential, ϕ, can be solved from the Laplace equation

$$\nabla^2\phi = 0 \tag{7}$$

with the channel walls and particle surface being electrically insulating. The externally supplied voltages were imposed to the electrode surfaces in the end-channel reservoirs. Other assumptions that were made in this model include the following: (1) fluid properties remain uniform throughout the channel, which is valid when Joule heating effects are insignificant;[57] (2) particle inertia is negligible because of the small Reynolds number;[58] (3) the rotation of a particle is small or does not affect its translation; and (4) particle−particle interactions are neglected for dilute particle solutions.

RESULTS AND DISCUSSION

Binary Particle Separation. Figure 3 demonstrates a continuous-flow electrokinetic separation of 5 and 10 μm diameter particles in the T-shaped microchannel via the wall-induced electrical lift. The two inlet reservoirs for the particle mixture and sheath fluid (see Figure 1) are imposed with 600 and 1275 V DC voltages, respectively, and the outlet reservoir

DOI: 10.1021/la5045464
Langmuir 2015, 31, 620−627

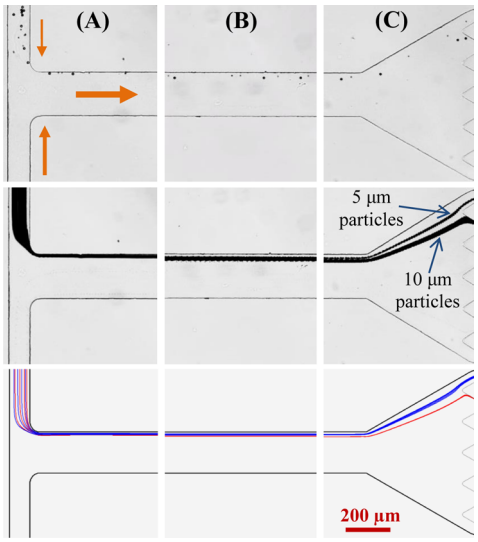

Figure 3. Demonstration of a continuous-flow electrokinetic separation of 5 and 10 μm diameter particles in a T-shaped microchannel using the wall-induced non-inertial lift force: (top row) snapshot image, (middle row) superimposed image, and (bottom row) theoretically predicted trajectories (blue and red lines are for 5 and 10 μm particles, respectively) at the (A) entrance, (B) middle, and (C) exit of the main branch. The two inlet reservoirs for the particle mixture and sheath fluid (see Figure 1) are imposed with 600 and 1275 V DC voltages, respectively, and the outlet reservoir is grounded. The block arrows on the images in the top row indicate the flow directions.

is grounded. The resulting electric field in the main branch is about 536 V/cm, which can be obtained from either the analysis of the equivalent electric circuit for the fluids[59] (see Appendix A) or the numerical model. At this electric field, Joule heating effects in the tested solution were found insignificant.[31,32] It is because the induced fluid temperature rise, ΔT, was estimated to be less than 0.5 °C via $\Delta T = \sigma E^2 l^2/k$, where σ and k are the fluid electrical (=210 μS/cm, experimentally measured) and thermal (=0.6 W m^{-1} K^{-1}, assumed equal to that of water) conductivities and l is the hydraulic diameter of the channel with a calculated value of 67 μm.[57] The electric field ratio between the sheath fluid and particle mixture side branches is 11.5. Attributed to the plug-like electrokinetic flow profile under the thin electric double layer assumption,[6,7] the stream width ratio of the sheath fluid to particle mixture should also be 11.5 in the main branch.[59] Thus, the focused particle stream width in the main branch can be calculated as 16.0 μm, which is consistent with the experimental images at the T junction, as viewed from Figure 3A (snapshot in the top row and superimposed in the middle row). Because this width is greater than the size of the larger particles to be separated, the centers of 5 and 10 μm particles should overlap and, hence, cannot be separated by solely the steric effects in traditional PFF.[47−49]

However, because of the wall-induced electrical lift force, particles are deflected away from the sidewall of the main branch at a particle size-dependent rate, i.e., eq 3. This leads to a gradually increased displacement between 5 and 10 μm particles, which is illustrated in Figure 3B with the snapshot (top row) and superimposed (middle row) images taken in the middle of the main branch. The result is a continuous-flow separation of particles by size into different flow paths at the outlet of the channel, as shown in Figure 3C. The numerically predicted trajectories of the two types of particles are also presented in Figure 3 (see the bottom row) at exactly the experimental conditions, which agree reasonably well with the experimentally obtained images in the middle row. A quantitative comparison between the experiment and simulation results is presented in the following sections. Note that, because particles are treated as massless points in the simulation, the width of the numerically predicted particle stream cannot be compared directly to that in the superimposed images.

Effect of the Electric Field Ratio in between the Two Side Branches. The effect of the electric field ratio in between the two side branches on the particle separation in the T-shaped microchannel is studied by fixing the DC voltage onto the particle mixture reservoir (see Figure 1), $\phi_{particle}$, at 600 V while varying that onto the sheath fluid reservoir, ϕ_{sheath}, from 1115 to 1320 V. Table 1 presents the electric field ratios

Table 1. Calculated Electric Field Ratio in between the Sheath Fluid and Particle Mixture Side Branches and Particle Stream Width in the Main Branch of the T-Shaped Microchannel[a]

$\phi_{particle}$ (V)	ϕ_{sheath} (V)	ratio of the electric field	particle stream width (μm)
600	1115	5.7	29.9
600	1200	8.0	22.2
600	1275	11.5	16.0
600	1320	15.0	12.5

[a] $\phi_{particle}$ and ϕ_{sheath} represent the DC voltages imposed to the reservoirs for the particle mixture and sheath fluid (see Figure 1), respectively.

between the sheath fluid and particle mixture side branches and the corresponding particle stream widths in the main branch (immediately after the T junction). All listed values were determined from an equivalent electric circuit analysis of the fluids in the channel[59] (see Appendix A). For all four tested values of ϕ_{sheath}, the width of the focused particle stream is greater than 10 μm, indicating that the steric-effect-enabled PFF[47−49] alone is unable to separate 10 μm particles from 5 μm particles.

Figure 4A compares the experimentally obtained (right half of each panel) and numerically predicted (left half of each panel, mirrored horizontally) trajectories of 5 and 10 μm particles at the T junction (top row) and channel outlet (bottom row) for the four tested cases. With the increase of ϕ_{sheath} or electric field ratio (see Table 1), both sizes of particles become better focused in the main branch and, in turn, an enhanced separation, as demonstrated in Figure 4A (from left to right). This trend is apparent in both the experimental and numerical images, which agree reasonably well. At the smallest electric field ratio, the substreams of 5 and 10 μm particles overlap a bit (clearly viewed from the numerical simulation on the bottom left image), leading to an incomplete separation. With the increasing electric field ratio, the exiting streams of both types of particles become thinner (more obvious for 5 μm particles) and, moreover, are separated further apart. Figure 4B shows a quantitative comparison of the experimentally measured (symbols) and numerically predicted (lines) relative positions (with respect to the right-most sidewall at the tip of the embedded blocks) of the separated particles at the channel outlet. Error bars are included for the experimental data to

DOI: 10.1021/la5045464
Langmuir 2015, 31, 620−627

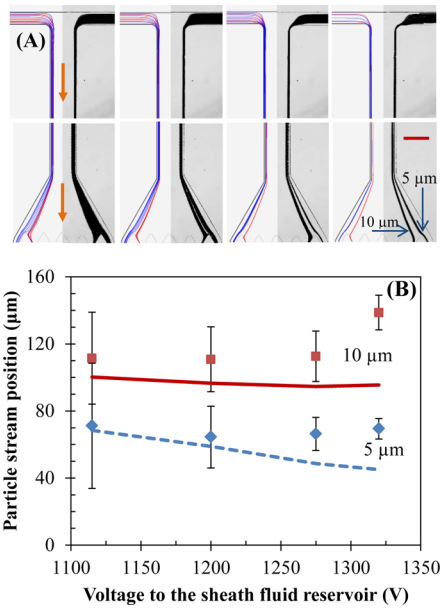

Figure 4. Electric field ratio effect on the electrokinetic separation of 5 and 10 μm particles in the T-shaped microchannel via the wall-induced electrical lift force: (A) numerical (left half in each panel, mirrored horizontally) and experimental (right half) images illustrating the particle focusing at the T junction (top row) and particle separation at the channel outlet (bottom row) and (B) line graph comparing the numerically predicted (lines) and experimentally measured (symbols) relative positions (with respect to the right-most sidewall at the tip of the embedded blocks) of the separated particles at the channel outlet. The DC voltage imposed to the reservoir for sheath fluid (see Figure 1) is varied from 1115 to 1200, 1275, and 1320 V from left to right in panel A. The voltage to the reservoir for the particle mixture is fixed at 600 V. The corresponding electric field ratios between the sheath fluid and particle mixture side branches are referred to Table 1. Note that the blue and red lines are for 5 and 10 μm particles in all numerical images. The block arrows in panel A indicate the flow directions. The scale bar on the bottom right image of panel A represents 200 μm.

cover the span of the particle stream width with respect to its center. The enhanced displacement between 5 and 10 μm particles is apparent in both the experimental and simulation results when the electric field ratio is increased. However, the deflection of each type of particles is underestimated, especially significant at high electric field ratios. This deviation may arise from the lateral drift velocity of a particle in eq 2 being obtained for particles far away from a planar wall and at the leading order only.[28]

Effect of the Electric Field Magnitude in the Main Branch. The effect of the electric field magnitude in the main branch on the electrokinetic particle separation in the T-shaped microchannel is examined by varying the DC voltage imposed to the particle mixture reservoir, $\phi_{particle}$, from 200 to 400, 600, and 800 V, while the electric field ratio in between the sheath fluid and particle mixture side branches is maintained at 11.3. Note this is the same ratio as that used in Figure 3, where $\phi_{particle}$ = 600 V and ϕ_{sheath} = 1275 V. The calculated electric field magnitudes in the main branch are 179, 353, 536, and 715 V/cm in order. In all four cases, the particle mixture is equally focused at the T junction (data not shown) because of the identical electric field ratio between the two side branches. This can be viewed from the nearly unvaried stream widths of both 5 and 10 μm particles among the four tested cases in Figure 5A. However, the particle deflection in eq 3 increases with the

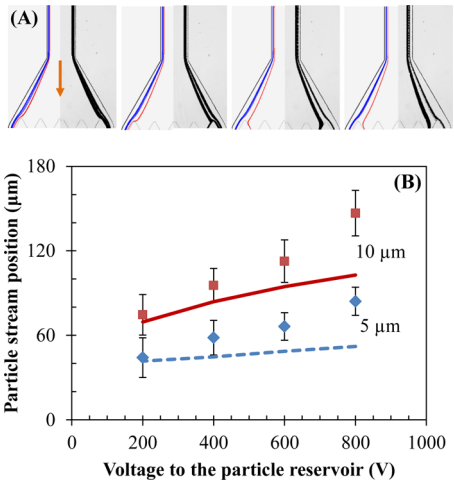

Figure 5. Effect of the electric field magnitude in the main branch on the electrokinetic separation of 5 and 10 μm particles in the T-shaped microchannel via the wall-induced electrical lift force: (A) numerical (left half in each panel, mirrored horizontally) and experimental (right half) images illustrating the particle separation at the channel outlet and (B) line graph comparing the numerically predicted (lines) and experimentally measured (symbols) relative positions (with respect to the right-most sidewall at the tip of the embedded blocks) of the separated particles at the channel outlet. The DC voltage imposed to the reservoir for the particle mixture is varied from 200 to 400, 600, and 800 V from left to right in panel A. The electric field ratio between the sheath fluid and particle mixture side branches (see Figure 1) is maintained at 11.3. Note that the blue and red lines are for 5 and 10 μm particles in all numerical images. The block arrow in panel A indicates the flow direction.

increasing electric field and so does the displacement between the two types of particles. Such an enhanced particle separation is demonstrated by the consistent experimental (right half of each panel) and numerical (left half, mirrored horizontally) images in Figure 5A. The quantitative comparison between the experimentally measured (symbols) and numerically predicted (lines) relative positions of the 5 and 10 μm particle streams at the channel outlet is illustrated in Figure 5B. Similar to what we see in Figure 4B, the numerical model correctly predicts the enhanced separation distance between the two types of particles with the increase of the electric field but still underestimates the deflection of each type.

Ternary Particle Separation. Figure 6 demonstrates a continuous-flow ternary separation of 3, 5, and 10 μm particles in the T-shaped microchannel via the wall-induced non-inertial lift in electrokinetic flow. The DC voltages imposed to the reservoirs for particle mixture and sheath fluid are 600 and 1320 V, respectively. This generates an average electric field of 549 V/cm in the main branch and an electric field ratio of 15 between the two side branches. Accordingly, the particle mixture is pinched by the sheath fluid to a stream of 12.5 μm wide (see Table 1) at the T junction, which is still greater than the size of the largest particles. Therefore, the three types of particles cannot be separated by the steric-effect-based PFF[47−49] alone, as explained above. However, the lateral migration because of the wall-induced electrical lift in electrokinetic flow (eq 3) depends highly upon particle size, yielding a continuously increased displacement among the particles along the length of the main branch. This results in a clear separation into three substreams at the channel outlet as seen from the experimental (left for snapshot and middle for

DOI: 10.1021/la5045464
Langmuir 2015, 31, 620−627

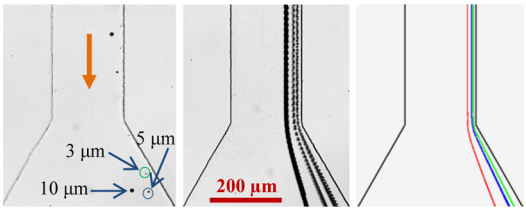

Figure 6. Continuous-flow ternary separation of 3, 5, and 10 μm diameter particles in a T-shaped microchannel via the wall-induced electrical lift force in electrokinetic flow: (left) snapshot image, (middle) superimposed image, and (right) theoretically predicted trajectories (green, blue, and red lines are for 3, 5, and 10 μm particles, respectively) at the channel outlet. The two inlet reservoirs for the particle mixture and sheath fluid (see Figure 1) are imposed with 600 and 1320 V DC voltages, respectively, and the outlet reservoir is grounded. The block arrow on the left image indicates the flow direction.

superimposed) and numerical (right) images in Figure 6. It is important to point out that the T microchannel used in this work has not been optimized, for which a reduced width and/or an increased length of the main branch is expected to enhance the particle separation significantly.

CONCLUSION

We have developed a continuous-flow electrokinetic method that exploits the wall-induced non-inertial lift to separate particles by intrinsic properties. Such an electrically originated lift force arises from the asymmetric electric field around a particle in the transverse direction when the particle moves eccentrically through a straight microchannel. The resulting lateral deflection is an explicit function of both particle size and surface charge, as seen from eq 3. This method has been demonstrated through both a binary separation of 5/10 μm particles and a ternary separation of 3/5/10 μm particles in a T-shaped microchannel. Also, the effects of the electric field ratio between the two side branches and the electric field magnitude in the main branch are both examined. Moreover, we have developed a semi-analytical model to simulate the electrokinetic particle transport and separation, whose predictions agree reasonably well with the experimental images, although the particle deflection is underestimated at strong electric fields because of the limitations of eq 2. Our proposed particle separation method has several advantages over the traditional steric-effect-based PFF[47−49] method: (1) particles do not need to be strictly aligned against a wall such that the consumption of sheath fluid is reduced; (2) the wall-induced electrical lift increases the lateral particle displacement such that the separation efficiency is enhanced; and (3) the pinched branch (i.e., the main branch of our T channel) does not need to be small to distinctly distinguish the relative position of particle centers such that the channel is less prone to clogging.

APPENDIX A: EQUIVALENT ELECTRIC CIRCUIT ANALYSIS OF FLUIDS IN A T-SHAPED MICROCHANNEL

The equivalent electric circuit of fluids in the tested T-shaped microchannel is schematically shown in Figure A1, where $R_{\text{side branch}} = L_{\text{side branch}}/\sigma W_{\text{side branch}}D$ and $R_{\text{main branch}} = L_{\text{main branch}}/\sigma W_{\text{main branch}}D$ represent the electrical resistances of the fluids in the side and main branches with L, W, and D denoting the branch length, width, and depth, respectively.

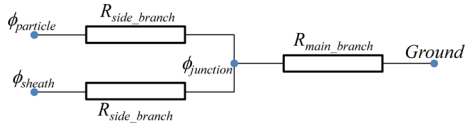

Figure A1. Equivalent electric circuit of fluids in the tested T-shaped microchannel where R represents the electrical resistance.

Considering the conservation of electric current through the microchannel, one can easily obtain

$$\frac{\phi_{\text{particle}} - \phi_{\text{junction}}}{R_{\text{side branch}}} + \frac{\phi_{\text{sheath}} - \phi_{\text{junction}}}{R_{\text{side branch}}} = \frac{\phi_{\text{junction}}}{R_{\text{main branch}}} \tag{A1}$$

which then gives rise to

$$\phi_{\text{junction}} = \frac{\phi_{\text{particle}} + \phi_{\text{sheath}}}{2 + L_{\text{side branch}}W_{\text{main branch}}/L_{\text{main branch}}W_{\text{side branch}}} = \frac{\phi_{\text{particle}} + \phi_{\text{sheath}}}{3.5} \tag{A2}$$

As such, the average electric field in the main branch of the T-shaped microchannel is

$$E_{\text{main branch}} = \frac{\phi_{\text{particle}} + \phi_{\text{sheath}}}{3.5L_{\text{main branch}}} \tag{A3}$$

and the electric field ratio between the sheath fluid and particle mixture side branches is given by

$$\frac{E_{\text{sheath}}}{E_{\text{particle}}} = \frac{2.5\phi_{\text{sheath}} - \phi_{\text{particle}}}{2.5\phi_{\text{particle}} - \phi_{\text{sheath}}} \tag{A4}$$

The calculated values of the electric field ratio, $E_{\text{sheath}}/E_{\text{particle}}$, for the voltages used in our experiments are listed in Table 1. Also listed are the particle stream widths in the main branch that were simply calculated from $W_{\text{main branch}}/(1 + E_{\text{sheath}}/E_{\text{particle}})$ considering the plug-like electroosmotic fluid velocity.

AUTHOR INFORMATION

Corresponding Authors

*E-mail: jphsu@ntu.edu.tw.

*E-mail: xcxuan@clemson.edu.

Notes

The authors declare no competing financial interest.

ACKNOWLEDGMENTS

This work was partially supported by Clemson University through a departmental Small Grants for Exploratory Research (SGER) grant to Xiangchun Xuan.

REFERENCES

(1) Pamme, N. Continuous flow separations in microfluidic devices. *Lab Chip* **2007**, *7*, 1644−1659.

(2) Gossett, D. R.; Weaver, W. M.; Mach, A. J.; Hur, S. C.; Tse, H. T.; Lee, W.; Amini, H.; Di Carlo, D. Label-free cell separation and sorting in microfluidic systems. *Anal. Bioanal. Chem.* **2010**, *397*, 3249−3267.

(3) Lenshof, A.; Laurell, T. Continuous separation of cells and particles in microfluidic systems. *Chem. Soc. Rev.* **2010**, *39*, 1203−1217.

(4) Watarai, H. Continuous separation principles using external microaction forces. *Annu. Rev. Anal. Chem.* **2013**, *6*, 353−378.

DOI: 10.1021/la5045464
Langmuir 2015, 31, 620−627

(5) Sajeesh, P.; Sen, A. K. Particle separation and sorting in microfluidic devices: A review. *Microfluid. Nanofluid.* **2014**, *17*, 1−52.
(6) Li, D. *Electrokinetics in Microfluidics*; Elsevier Academic Press: Burlington, MA, 2014.
(7) Chang, H. C.; Yeo, L. Y. *Electrokinetically Driven Microfluidics and Nanofluidics*; Cambridge University Press: Cambridge, U.K., 2009.
(8) Pethig, R. Review article—Dielectrophoresis: Status of the theory, technology, and applications. *Biomicrofluidics* **2010**, *4*, 022811.
(9) Kim, S. B.; Yoon, S. Y.; Sung, H. J.; Kim, S. S. Cross-type optical particle separation in a microchannel. *Anal. Chem.* **2008**, *80*, 2628−2630.
(10) Ding, X.; Li, P.; Lin, S. C.; Stratton, Z. S.; Nama, N.; Guo, F.; Slotcavage, D.; Mao, X.; Shi, J.; Costanzo, F.; Huang, T. J. Surface acoustic wave microfluidics. *Lab Chip* **2013**, *13*, 3626−3649.
(11) Liang, L.; Xuan, X. Continuous sheath-free magnetic separation of particles in a U-shaped microchannel. *Biomicrofluidics* **2012**, *6*, 044106.
(12) Maenaka, H.; Yamada, M.; Nakashima, M.; Seki, M. Continuous and size-dependent sorting of emulsion droplets using hydrodynamics in pinched microchannels. *Langmuir* **2008**, *24*, 4405−4410.
(13) Martel, J. M.; Toner, M. Inertial focusing in microfluidics. *Annu. Rev. Biomed. Eng.* **2014**, *16*, 371−396.
(14) Amini, H.; Lee, W.; Di Carlo, D. Inertial microfluidic physics. *Lab Chip* **2014**, *14*, 2739−2761.
(15) Huang, L.; Cox, E. C.; Austin, R. H.; Sturm, J. C. Continuous particle separation through deterministic lateral displacement. *Science* **2004**, *304*, 987−990.
(16) Choi, S.; Song, S.; Choi, C.; Park, J. K. Microfluidic self-sorting of mammalian cells to achieve cell cycle synchrony by hydrophoresis. *Anal. Chem.* **2009**, *81*, 1964−1968.
(17) Lapizco-Encinas, B. H.; Simmons, B. A.; Cummings, E. B.; Fintschenko, Y. Insulator-based dielectrophoresis for the selective concentration and separation of live bacteria in water. *Electrophoresis* **2004**, *25*, 1695−1704.
(18) Hawkins, B. G.; Smith, A. E.; Syed, Y. A.; Kirby, B. J. Continuous-flow particle separation by 3D insulative dielectrophoresis using coherently shaped, DC-biased, AC electric fields. *Anal. Chem.* **2007**, *79*, 7291−7300.
(19) Pysher, M. D.; Hayes, M. A. Electrophoretic and dielectrophoretic field gradient technique for separating bioparticles. *Anal. Chem.* **2007**, *79*, 4552−4557.
(20) Patel, S.; Showers, D.; Vedantam, P.; Tzeng, T.; Qian, S.; Xuan, X. Microfluidic separation of live and dead yeast cells using reservoir-based dielectrophoresis. *Biomicrofluidics* **2012**, *6*, 034102.
(21) Lewpiriyawong, N.; Yang, C. Continuous separation of multiple particles by negative and positive dielectrophoresis in a modified H-filter. *Electrophoresis* **2014**, *35*, 714−720.
(22) Church, C.; Zhu, J.; Xuan, X. Negative dielectrophoresis-based particle separation by size in a serpentine microchannel. *Electrophoresis* **2011**, *32*, 527−531.
(23) Zhu, J.; Xuan, X. Curvature-induced dielectrophoresis for continuous separation of particles by charge in spiral microchannels. *Biomicrofluidics* **2011**, *5*, 024111.
(24) Li, M.; Li, W. H.; Zhang, J.; Alici, G.; Wen, W. A review of microfabrication techniques and dielectrophoretic microdevices for particle manipulation and separation. *J. Phys. D: Appl. Phys.* **2014**, *47*, 063001.
(25) DuBose, J.; Lu, X.; Patel, S.; Qian, S.; Joo, S.; Xuan, X. Microfluidic electrical sorting of particles based on shape in a spiral microchannel. *Biomicrofluidics* **2014**, *8*, 014101.
(26) Young, E.; Li, D. Dielectrophoretic force on a sphere near a planar boundary. *Langmuir* **2005**, *21*, 12037−12046.
(27) Kang, K.; Xuan, X.; Kang, Y.; Li, D. Effects of DC-dielectrophoretic force on particle trajectories in microchannels. *J. Appl. Phys.* **2006**, *99*, 064702.
(28) Yariv, E. "Force-free" electrophoresis? *Phys. Fluids* **2006**, *18*, 031702.
(29) Zhao, H.; Bau, H. H. On the effect of induced electro-osmosis on a cylindrical particle next to a surface. *Langmuir* **2007**, *23*, 4053−4063.
(30) Pohl, H. A. *Dielectrophoresis: The Behavior of Neutral Matter in Non-uniform Electric Fields*; Cambridge University Press: Cambridge, U.K., 1978.
(31) Liang, L.; Ai, Y.; Zhu, J.; Qian, S.; Xuan, X. Wall-induced lateral migration in particle electrophoresis through a rectangular microchannel. *J. Colloid Interface Sci.* **2010**, *347*, 142−146.
(32) Liang, L.; Qian, S.; Xuan, X. Three-dimensional electrokinetic particle focusing in a rectangular microchannel. *J. Colloid Interface Sci.* **2010**, *350*, 377−379.
(33) Kazoe, Y.; Yoda, M. Experimental study of the effect of external electric fields on interfacial dynamics of colloidal particles. *Langmuir* **2011**, *27*, 11481−11488.
(34) DuBose, J.; Zhu, J.; Patel, S.; Lu, X.; Tupper, N.; Stonaker, J. M.; Xuan, X. Electrokinetic particle separation in a single-spiral microchannel. *J. Micromech. Microeng.* **2014**, *24*, 115018.
(35) Liang, Q.; Zhao, C.; Yang, C. Enhancement of electrophoretic mobility of microparticles near a solid wall—Experimental verification. *Electrophoresis* **2014**, DOI: 10.1002/elps.201400405.
(36) Lu, X.; Patel, S.; Zhang, M.; Joo, S. W.; Qian, S.; Ogale, A.; Xuan, X. An unexpected particle oscillation for electrophoresis in viscoelastic fluids through a microchannel constriction. *Biomicrofluidics* **2014**, *8*, 021802.
(37) Cheng, N. Formula for the viscosity of a glycerol−water mixture. *Ind. Eng. Chem. Res.* **2008**, *47*, 3285−3288.
(38) Yariv, E.; Brenner, H. The electrophoretic mobility of a closely fitting sphere in a cylindrical pore. *SIAM J. Appl. Math.* **2004**, *64.2*, 423−441.
(39) Ye, C.; Sinton, D.; Erickson, D.; Li, D. Electrophoretic motion of a circular cylindrical particle in a circular cylindrical microchannel. *Langmuir* **2002**, *18*, 9095−9101.
(40) Tseng, S.; Cho, C. H.; Chen, Z. S.; Hsu, J.P. Electrophoresis of an ellipsoid along the axis of a cylindrical pore: Effect of a charged boundary. *Langmuir* **2008**, *24*, 2929−2937.
(41) Yariv, E.; Brenner, H. Near-contact electrophoretic motion of a sphere parallel to a planar wall. *J. Fluid Mech.* **2003**, *484*, 85−111.
(42) Xuan, X.; Ye, C.; Li, D. Near-wall electrophoretic motion of spherical particles in cylindrical capillaries. *J. Colloid Interface Sci.* **2005**, *289*, 286−290.
(43) Russel, W. B.; Saville, D. A.; Schowalter, W. R. *Colloidal Dispersions*; Cambridge University Press: Cambridge, U.K., 1992.
(44) Bike, S. G.; Prieve, D. C. Electrokinetic lift of a sphere moving in slow shear flow parallel to a wall: II. Theory. *J. Colloid Interface Sci.* **1995**, *175*, 422−434.
(45) Yariv, E.; Schnitzer, O.; Frankel, I. Streaming-potential phenomena in the thin-Debye-layer limit. Part 1. General theory. *J. Fluid Mech.* **2011**, *685*, 306−334.
(46) Schnitzer, O.; Frankel, I.; Yariv, E. Streaming-potential phenomena in the thin-Debye-layer limit. Part 2. Moderate Péclet numbers. *J. Fluid Mech.* **2012**, *704*, 109−136.
(47) Kawamata, T.; Yamada, M.; Yasuda, M.; Seki, M. Continuous and precise particle separation by electroosmotic flow control in microfluidic devices. *Electrophoresis* **2008**, *29*, 1423−1430.
(48) Yamada, M.; Nakashima, M.; Seki, M. Pinched flow fractionation: continuous size separation of particles utilizing a laminar flow profile in a pinched microchannel. *Anal. Chem.* **2004**, *76*, 5465−5471.
(49) Takagi, J.; Yamada, M.; Yasuda, M.; Seki, M. Continuous particle separation in a microchannel having asymmetrically arranged multiple branches. *Lab Chip* **2005**, *5*, 778−784.
(50) Wu, Z.; Liu, A.; Hjort, K. Microfluidic continuous particle/cell separation via electroosmotic-flow-tuned hydrodynamic spreading. *J. Micromech. Microeng.* **2007**, *17*, 1992−1999.
(51) Vig, A. L.; Kristensen, A. Separation enhancement in pinched flow fractionation. *Appl. Phys. Lett.* **2008**, *93*, 203507.

DOI: 10.1021/la5045464
Langmuir 2015, 31, 620−627

(52) Nho, H. W.; Yoon, T. H. Enhanced separation of colloidal particles in an AsPFF device with a tilted sidewall and vertical focusing channels (t-AsPFF-v). *Lab Chip* **2013**, *13*, 773−776.
(53) Lee, K.; Kim, S.; Lee, K.; Sung, H. Enhancement by optical force of separation in pinched flow fractionation. *Lab Chip* **2011**, *11*, 354−357.
(54) Morijiri, M.; Sunahiro, S.; Senaha, M.; Yamada, M.; Seki, M. Sedimentation pinched-flow fractionation for size- and density-based particle sorting in microchannels. *Microfluid. Nanofluid.* **2011**, *11*, 105−110.
(55) Ai, Y.; Park, S.; Zhu, J.; Xuan, X.; Beskok, A.; Qian, S. DC electrokinetic particle transport in an L-shaped microchannel. *Langmuir* **2010**, *26*, 2937−2944.
(56) Ermolina, I.; Morgan, H. The electrokinetic properties of latex particles: Comparison of electrophoresis and dielectrophoresis. *J. Colloid Interface Sci.* **2005**, *285*, 419−428.
(57) Casterllanos, A.; Ramos, A.; Gonzalez, A.; Green, N. G.; Morgan, H. Electrohydrodynamics and dielectrophoresis in microsystems: Scaling laws. *J. Phys. D: Appl. Phys.* **2003**, *36*, 2584−2597.
(58) Happel, J.; Brenner, H. *Low Reynolds Number Hydrodynamics*; Noordhoff International Publishing: Leyden, Netherlands, 1973.
(59) Xuan, X.; Li, D. Focused electrophoretic motion and selected electrokinetic dispensing of particles and cells in cross-microchannels. *Electrophoresis* **2005**, *26*, 3552−3560.

DOI: 10.1021/la5045464
Langmuir 2015, 31, 620−627